Self-Association in Water of Copolymers of Acrylic Acid and *N*-Dodecylmethacrylamide As Studied by Fluorescence, Dynamic Light Scattering, and Rheological Techniques

Yoshiko Sato, Akihito Hashidzume, and Yotaro Morishima*

Department of Macromolecular Science, Graduate School of Science,Osaka University, Toyonaka, Osaka 560-0043, Japan

Received March 13, 2001; Revised Manuscript Received June 1, 2001

ABSTRACT: The self-association of random copolymers of acrylic acid (AA) and *N*-dodecylmethacrylamide (DodMAm) with 5.1−28.4 mol % DodMAm contents (f_{Dod}) in water was investigated by fluorescence, quasi-elastic light scattering (QELS), and rheological methods as a function of f_{Dod} and pH. The copolymers exhibited a strong tendency for interpolymer association, forming micelle-like multipolymer aggregates. This is a striking contrast to the previous finding that random copolymers of 2-(acrylamido)-2-methylpropanesulfonate (AMPS) and DodMAm exhibited a strong tendency for intrapolymer association, forming unimolecular micelles. At pH 10, the AA/DodMAm copolymers with a smaller f_{Dod} formed multipolymer aggregates with a larger size, the size decreasing with increasing f_{Dod}. At pH 4, this trend was opposite; the size of the multipolymer aggregate increased with increasing f_{Dod}. Independent of f_{Dod} and pH, the size of the multipolymer aggregates increased with increasing polymer concentration (C_p). The association behavior and the nature of multipolymer aggregates of the AA/DodMAm copolymers with small f_{Dod} values (≤9.1 mol %) were markedly different from those with larger f_{Dod} (≥12.8 mol %). As the pH was decreased, the size of the multipolymer aggregate decreased when $f_{Dod} \leq 9.1$ mol % whereas it increased when $f_{Dod} \geq 12.8$ mol %. Independent of f_{Dod}, the mean aggregation number (N_{agg}) of dodecyl groups in one hydrophobic microdomain decreased with decreasing pH. Multipolymer aggregates formed from the AA/DodMAm copolymer of a small f_{Dod} (9.1 mol %) at high C_p were more dynamic in nature than those from the copolymer of larger f_{Dod} (22.4 mol %), the former showing shear rate dependent viscosity behavior while the latter did not. On the basis of the characterization data, multipolymer association models for the AA/DodMAm copolymers were proposed.

Introduction

The spontaneous self-association of hydrophobically modified water-soluble polymers (amphiphilic polymers) in aqueous solution has been studied extensively over the past decades because of its academic as well as industrial importance.[1−3] Of particular interest is a class of amphiphilic polyelectrolytes that undergo hydrophobic associations competing with electrostatic repulsions to form various types of micelle-like nanostructures. It has been well-established that, in random copolymers of ionic and hydrophobic monomers, the types of ion-containing[4−9] and hydrophobe-containing[10−16] monomer units, copolymer composition,[10,11,16−21] sequence distribution of ionic and hydrophobic monomer units along the polymer chain,[18] and spacer between the hydrophobe and polymer backbone[16,22−27] are some of the important architectural parameters to determine the self-associative properties of the polymers. In earlier papers, we reported that random copolymers of sodium 2-(acrylamido)-2-methylpropanesulfonate (AMPS) and *N*-dodecylmethacrylamide (DodMAm) showed a strong preference for intrapolymer hydrophobic self-association in aqueous solutions independent of the polymer concentration, forming single macromolecular (unimolecular) micelles, even at high polymer concentrations.[13,20,21,28,29]

McCormick and co-workers[4−9,30] reported the influence of the nature of charged groups in anionic polymers on various solution properties such as rheological behavior, phase separation in the presence of divalent cations, and responsiveness to changes in pH and ionic strength. They compared self-association properties of terpolymers of acrylamide (AM), *n*-decylacrylamide (C10AM) (0.5 mol %), and sodium acrylate (NaAA), sodium 3-acrylamido-3-methylbutanoate (NaAMB), or NaAMPS and found that AM/C10AM/NaAA terpolymers exhibited a much stronger tendency for interpolymer hydrophobic association than did AM/C10AM/NaAMB and AM/C10AM/NaAMPS terpolymers.[4] Namely, they revealed that interpolymer hydrophobic associations occurred more favorably in polymers with charged groups located closer to the polymer backbone. In the NaAMB and NaAMPS units, charged groups are separated via several bonds from the backbone, allowing the charged groups to extend out farther from the backbone. Thus, the mobility and conformational freedom of the charged groups are pronouncedly large, reducing the charge density along the polymer chain.[5] In addition, the geminal dimethyl groups in the NaAMB and NaAMPS units in the AM/C10AM/NaAMB and AM/C10AM/NaAMPS terpolymers may be hydrophobic enough to interfere with interpolymer associations of *n*-decyl groups in the C10AM units in the terpolymers.[4] Furthermore, the favorable hydration of the secondary amide in the NaAMB and NaAMPS units may play an important role in the hydrophobic self-association of the polymers.

We were motivated by these important results reported by McCormick and co-workers[4−9,30] to investigate the association properties of copolymers of acrylic acid (AA) and DodMAm (Chart 1) in comparison with those of AMPS/DodMAm copolymers. In the present paper, we report on the self-association properties of AA/DodMAm copolymers with varying contents of DodMAm

10.1021/ma010446f CCC: $20.00
Published on Web 07/20/2001

Chart 1. AA/DodMAm Copolymer

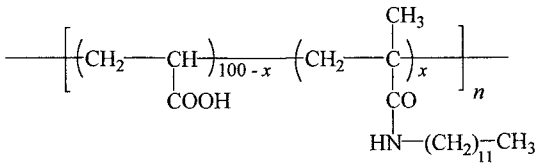

in aqueous solutions at varying pH. Some of the experimental results were compared with those of AMPS/DodMAm copolymers reported in our earlier papers.[13,16,20,21,28,29,31]

Experimental Section

Materials. *N*-Dodecylmethacrylamide (DodMAm) was prepared as reported previously.[31] Acrylic acid (AA) was purified by distillation under reduced pressure. 2,2′-Azobis(isobutyronitrile) (AIBN) was recrystallized from methanol. Pyrene was recrystallized twice from ethanol. Analytical grade NaCl was used without further purification. Other reagents were used as received. All the chemicals were purchased from Wako Pure Chemical Co. Milli-Q water was used to prepare polymer solutions.

Polymers. Copolymers of AA and DodMAm were prepared by free-radical polymerization initiated by AIBN in *N*,*N*-dimethylformamide (DMF). A mixture of AA, DodMAm, and 0.1 mol % (on the basis of the total monomer concentration) of AIBN was dissolved in DMF in a glass ampule, and the ampule was outgassed by six freeze−pump−thaw cycles on a high-vacuum line and sealed under high vacuum. The sealed ampule was immersed in a water bath of 60 °C for 15 h. The polymerization mixture was poured into a large excess of diethyl ether to precipitate resulting polymers. The polymer was purified by reprecipitation from a methanol solution into a large excess of diethyl ether and then dissolved in dilute aqueous NaOH. The alkaline solution was dialyzed against pure water for a week and finally lyophilized. Compositions of the copolymers were determined by elemental analysis (C/N ratio).

Copolymers of sodium 2-(acrylamido)-2-methylpropanesulfonate (AMPS) and DodMAm with DodMAm contents of 10 and 20 mol % are those prepared in our previous work.[21]

Measurements. a. Gel Permeation Chromatography (GPC). GPC measurements were performed at 40 °C with a JASCO GPC-900 system equipped with a Shodex Asahipak GF-7M HQ column in combination with JASCO UV-975 and RI-930 detectors. A 0.2 M $LiClO_4$ methanol solution was used as an eluent with an elution rate of 1.0 mL/min. The molecular weights were calibrated with standard poly(ethylene oxide) samples (Science Polymer Products, Inc.).

b. Titration. The potentiometric titration was performed using a Horiba F-23 pH meter equipped with a Horiba 6366-10D glass electrode. The reference electrode was calibrated with buffer solutions of pH 4, 7, and 9 prior to pH measurements. A 20 mL aqueous solution of polymer (3.0×10^{-2} M AA unit) containing 0.01 M HCl and 0.05 M NaCl was titrated with a 0.01 M NaOH standard solution, dispensed with a microburet, at 25 °C under a nitrogen atmosphere. The solution was equilibrated until each pH reading reaches a constant value.

c. Reduced Viscosity. Reduced viscosities of dilute polymer solutions were measured with a modified Ubbelohde type viscometer, with which the time of fall for pure water was 150 s at 25 °C. Sample solutions were prepared by dissolving a known amount of polymer in pure water or in a 0.05 M NaCl aqueous solution, and the polymer solutions were allowed to stand for 1 day for equilibration. The sample solutions were filtered with a 0.2 μm pore size membrane filter, and pH was adjusted to 4, 7, or 10 by adding an HCl or NaOH aqueous solution.

d. Absorption Spectra. Absorption spectra were recorded on a JASCO V-550 spectrophotometer using a 1.0 cm path length quartz cuvette. The concentrations of pyrene in sample solutions were calculated from the absorbance at 338 nm using $\epsilon_{338} = 37\,000$ M^{-1} cm^{-1} as the molar extinction coefficient.[32]

e. Steady-State Fluorescence. Steady-state spectra were recorded on a Hitachi F-4500 fluorescence spectrophotometer at room temperature. The slit widths for both the excitation and emission side were kept at 2.5 nm during measurement. Fluorescence emission spectra of pyrene were measured with excitation at 337 nm. Excitation spectra were monitored at 372 nm at varying pyrene concentrations to determine an apparent critical micelle concentration of the polymer, following the procedure reported by Wilhelm et al.[33]

f. Static Light Scattering (SLS). SLS data were obtained at 25 °C with an Otsuka Electronics Photal DLS-7000 light scattering spectrometer equipped with an Ar laser (output power = 55 mW at λ = 488 nm). Sample solutions were prepared by dissolving polymers in methanol containing 0.2 M $LiClO_4$, and the solutions were filtered with a 0.2 μm pore size membrane filter prior to SLS measurement. The optical constant (K) was calculated from the relation

$$K = \{4\pi^2 n^2 (\mathrm{d}n/\mathrm{d}c)^2\}/N_A\lambda^4 \quad (1)$$

where n is the refractive index of solution, N_A is Avogadro's number, λ is the wavelength, and $\mathrm{d}n/\mathrm{d}c$ is the refractive index increment against concentration. Values of $\mathrm{d}n/\mathrm{d}c$ were determined with an improved Schulz−Cantow type differential refractometer (Shimadzu). Apparent weight-average molecular weights (M_w) were estimated from the relation

$$Kc/R_\theta = 1/M_w(1 + 16\pi^2 n^2/3\lambda^2\langle S^2\rangle \sin^2(\theta/2) + ...) + 2A_2c + ... \quad (2)$$

where c is the polymer concentration, R_θ is the Rayleigh ratio, $\langle S^2\rangle$ is the mean-square radius of gyration, θ is the scattering angle, and A_2 is the second virial coefficient.

g. Quasi-Elastic Light Scattering (QELS). QELS data were obtained at varying scattering angles (50°−130°) at 25 °C with an Otsuka Electronics Photal DLS-7000 light scattering spectrometer equipped with an Ar laser lamp (output power = 60 mW at λ = 488 nm) and an ALV-5000 multi-τ-digital time correlator.

The intensity autocorrelation function, $g^{(2)}(t)$, is related to the normalized electric field autocorrelation function, $g^{(1)}(t)$, as

$$g^{(2)}(t) = B[1 + \beta|g^{(1)}(t)|^2] \quad (3)$$

where β is a constant parameter for an optical system and B is a baseline term. To obtain the relaxation time distribution, $\tau A(\tau)$, the inverse Laplace transform analysis for $g^{(2)}(t)$ was performed by conforming the REPES algorithm[34] as follows:

$$g^{(1)}(t) = \int \tau A(\tau) \exp(-t/\tau)\, \mathrm{d} \ln \tau \quad (4)$$

The relaxation time distributions are presented as a $\tau A(\tau)$ vs $\log \tau$ profile. The diffusion coefficient (D) was calculated from the relaxation rate (Γ) as

$$D = (\Gamma/q^2)_{q\to 0} \quad (5)$$

where q represents the magnitude of scattering vector expressed as $q = (4\pi n/\lambda)\sin(\theta/2)$, where n is the refractive index of the solvent. The hydrodynamic radius (R_h) was calculated using the Einstein−Stokes relation

$$R_h = k_B T/6\pi\eta D \quad (6)$$

where k_B is Boltzmann's constant, T is the absolute temperature, and η is the solvent viscosity.

h. Determination of Aggregation Number (N_{agg}). N_{agg} of polymer-bound dodecyl groups in the hydrophobic microdomain was determined by a fluorescence method using pyrene probes. Fluorescence decays for pyrene probes solubilized in

polymer solutions were measured by a time-correlated single-photon counting technique using a Horiba NAES 550 system equipped with a flash lamp filled with H_2. This system allows us to measure decay and response functions simultaneously. Pyrene probes were excited at 343 nm, and fluorescence was monitored at a wavelength in the neighborhood of 400 nm through combined band-pass (Toshiba KL-40) and cutoff (Toshiba L-38) filters. The decay data were analyzed by a conventional deconvolution technique. Sample solutions were purged with Ar for about 30 min prior to measurement. Monomeric pyrene fluorescence decay data were fitted to a kinetic model proposed by Infelta[35,36] and Tachiya[37] in the form of

$$\ln[I(t)/I(0)] = A_3[\exp(-A_4 t) - 1] - A_2 t$$

$$A_2 = k_0 + n_Q k_Q k^-/(k_Q + k^-)$$

$$A_3 = n_Q {k_Q}^2/(k_Q + k^-)^2$$

$$A_4 = k_Q + k^- \qquad (7)$$

where $I(t)$ and $I(0)$ are the fluorescence intensities at time t and 0 following pulse excitation, respectively, k_Q is the pseudo-first-order rate constant for quenching of the photoexcited pyrene, k_0 ($=\tau_0^{-1}$) is the fluorescence decay rate constant for pyrene inside the hydrophobic microdomain without excimer formation, n_Q is the mean number of quenchers dissolved in one hydrophobic microdomain, and k^- is the first-order rate constant for the exit of pyrene molecules from the microdomain. For criteria for the goodness of the fit, χ^2 and the weighted residuals were used. n_Q can be expressed as

$$n_Q = (A_3 A_4 + A_2 - k_0)^2/A_3 {A_4}^2 = [Q]_m/[M] \qquad (8)$$

where $[Q]_m$ is the molar concentration of quencher inside the hydrophobic microdomain and [M] is the molar concentration of the hydrophobic microdomain. Because the quenching of monomeric pyrene fluorescence is due to the excimer formation of pyrene, $[Q]_m$ corresponds to the concentration of pyrene. Thus, N_{agg} can be calculated from the $[Q]_m/[M]$ ratio.

i. Rheological Measurements. Steady-shear viscosities of polymer solutions at varying shear rates were measured with a DynAlyser 100 stress-control rheometer (RheoLogica) equipped with a cone and plate at 25 °C. The radius of the cone is 40 mm, and the angle between the cone and plate is 4.0°.

j. NMR. Two-dimensional nuclear Overhauser effect (NOE) spectroscopy (NOESY) data were obtained for the AMPS/DodMAm copolymer with a Varian UNITY-600 spectrometer in D_2O at 30 °C using a standard pulse sequence. Mixing time before the acquisition of free induction decay was carefully varied and fixed to 50 ms to obtain a genuine NOE and to avoid the effect of spin diffusion. Chemical shifts in all data were determined using tetramethylsilane as an internal standard.

k. Preparation of Sample Solutions. Sample solutions for fluorescence and QELS measurements were prepared as follows: Solid polymer samples (recovered by a freeze-drying technique from their aqueous solutions) were dissolved in pure water or in pyrene-saturated water, and the solutions were heated at ca. 90 °C for ca. 15 min. Pyrene-saturated water was prepared as reported previously.[22] After cooling the solutions to room temperature, a predetermined amount of NaCl was added to the polymer solutions to 0.05 M, and the solutions were heated at ca. 90 °C for ca. 15 min again. The solutions were allowed to stand for 1 day for equilibration. The pH of the sample solutions was adjusted to 4, 7, or 10 with a small amount of a 10 M HCl or NaOH aqueous solution prior to measurement. All sample solutions were filtered with a 0.2 or 0.45 μm membrane filter prior to measurement.

Results

Basic Characteristics of the Copolymers. Monomer reactivity ratios for AA (M_1) and DodMAm (M_2) in *N*,*N*-dimethylformamide at 60 °C were determined by fitting copolymer composition data to the copolymer composition equation. The monomer reactivity ratios thus determined are $r_1 = 0.73 \pm 0.16$ and $r_2 = 1.22 \pm 0.28$. These values indicate that the sequence distribution of AA and DodMAm units along the polymer chain is virtually random.

Table 1. Characteristics of AA/DodMAm Copolymers

DodMAm (mol %)		M_w[a] ($\times 10^4$)	M_w/M_n[a]	M_w[b] ($\times 10^4$)	no. of hydrophobes per polymer chain	apparent cmc[c] ($\times 10^{-3}$ g/L)	
feed	copolymer					pH 7	pH 4
0	0	1.1	1.69				
5.1	5.1						
9.9	9.1	0.9	2.64	3.2	3	7.0	7.1
14.9	12.8	1.6	3.14	2.0	6	6.2	5.3
20.0	22.4	2.4	3.17	2.3	13	6.2	2.0
29.9	28.4	1.8	2.56	2.2	15	5.9	1.5
39.7	42.9[d]						
48.8	50.4[d]						

[a] Determined by GPC using methanol containing 0.2 M $LiClO_4$ as eluent. [b] Determined by SLS in methanol containing 0.2 M $LiClO_4$. [c] Determined from steady-state fluorescence excitation spectra of pyrene probes. [d] Insoluble in water at all pH values.

In Table 1 are listed weight-average molecular weights (M_w) and the ratios of M_w to the number-average molecular weight (M_n) for four selected samples of the AA/DodMAm copolymers and reference poly(acrylic acid) (PAA) estimated by gel permeation chromatography (GPC). Values of M_w for the four samples estimated by static light scattering (SLS) are also listed in Table 1 for comparison. All the measurements of GPC and SLS were performed in methanol in which the polymers are expected to exist as a single molecular state (unimer) without association. The values of M_w determined by SLS and GPC are in fair agreement, being on the order of 10^4 independent of f_{Dod}. Therefore, M_n values estimated by GPC may be regarded as reasonably correct values. From f_{Dod} and M_n values, the number of DodMAm units per polymer chain was roughly calculated for the four selected copolymers as listed in Table 1. The copolymers with $f_{Dod} \leq 22.4$ mol % are soluble in water at pH $\geq$ 4, whereas the copolymer of $f_{Dod} = 28.4$ mol % exhibits a limited solubility at pH 4, being soluble only up to a polymer concentration (C_p) of 1 g/L at pH 4. The copolymers with $f_{Dod} \geq 42.9$ mol % were found to be insoluble in water at all pH values.

Acid−base equilibrium in hydrophobically modified poly(carboxylic acid)s may be influenced by polymer-bound hydrophobes in the vicinity of carboxyl groups. It is important to know the degree of dissociation, i.e., the charge density of the polymer, when one discusses the self-association behavior of hydrophobically modified poly(carboxylic acid)s at a given pH. Potentiometric titration curves for the AA/DodMAm copolymers with various f_{Dod} are shown in Figure 1, where the degree of dissociation (α) is plotted against solution pH. For the reference PAA, pH at a 50% dissociation (i.e., $\alpha = 0.5$) is ca. 5.8, whereas for the AA/DodMAm copolymer, pH at $\alpha = 0.5$ shifts slightly to higher pH values with increasing f_{Dod}. These observations indicate that the AA unit in the AA/DodMAm copolymer becomes slightly less acidic with increasing f_{Dod} in the copolymer.

In this work, we investigated the self-association behavior of the AA/DodMAm copolymer in aqueous solution at pH 4, 7, and 10. At pH 10, all the copolymers are almost fully dissociated ($\alpha \approx 1.0$) whereas they remain almost fully protonated ($\alpha \approx 0$) at pH 4. At pH

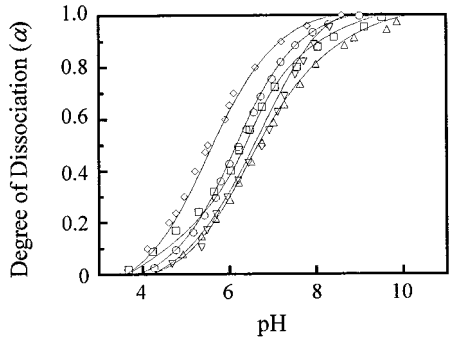

Figure 1. Potentiometric titration curves for PAA (◇) and AA/DodMAm copolymers with f_{Dod} = 9.1 (○), 12.8 (□), 22.4 (△), and 28.4 mol % (▽) in 0.05 M NaCl aqueous solutions.

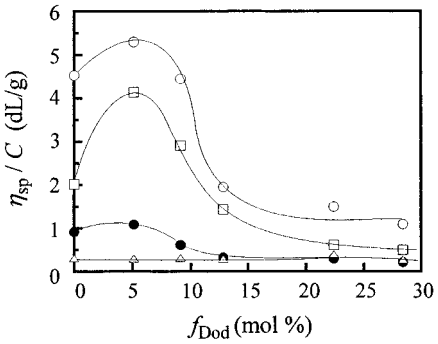

Figure 2. Reduced viscosity at C_p = 0.1 g/dL as a function of f_{Dod} at pH 4 (△), 7 (□), and 10 (○) in the absence of salt and at pH 10 (●) in the presence of 0.05 M NaCl.

7, α depends on f_{Dod}; i.e., α ≈ 0.9 for PAA while α ≈ 0.8, 0.7, 0.6, and 0.6 for the copolymers with f_{Dod} = 9.1, 12.8, 22.4, and 28.4 mol %, respectively.

Figure 2 shows the reduced viscosities at C_p = 0.1 g/dL measured at pH 4, 7, and 10 in salt-free aqueous solutions plotted as a function of f_{Dod}. For comparison, the reduced viscosities at pH 10 in 0.05 M NaCl aqueous solutions are also plotted as a function of f_{Dod}. At pH 4, viscosity is extremely low and apparently independent of f_{Dod}. As pH is increased to 7, viscosity increases greatly, especially near f_{Dod} = 5.1 mol %. It is to be noted that reduced viscosity values for the AA/DodMAm copolymer of f_{Dod} = 5.1 mol % at pH 7 and 10 are significantly larger than those for PAA (values at f_{Dod} = 0 mol % in Figure 2). This observation suggests the presence of interpolymer associations in the copolymer of f_{Dod} = 5.1 mol %, as will be discussed later. For f_{Dod} ≥ 5.1 mol %, viscosity decreases with increasing f_{Dod} at pH ≥ 7. This decrease occurs most significantly in an f_{Dod} region of 5.1−12.8 mol %. The copolymers with f_{Dod} = 22.4 and 28.4 mol % show very low viscosities that are much less dependent on pH compared with copolymers of lower f_{Dod}. This means that polymer chains adopt a collapsed conformation at f_{Dod} = 22.4 and 28.4 mol %, the collapse occurring most significantly in an f_{Dod} region of 5.1−12.8 mol %. When f_{Dod} < 13 mol % at pH 10, the addition of a small amount of NaCl causes a substantial decrease in the reduced viscosity, indicating that polymer chains collapse as a result of an electrostatic shielding of charges.

Hydrophobic Microdomains Formed by Dodecyl Groups. In aqueous solutions of amphiphilic polymers, pyrene is solubilized into hydrophobic domains, showing an increase in the ratio of the intensities of the third to first vibronic bands (I_3/I_1) in pyrene fluorescence spectra.[38−42]

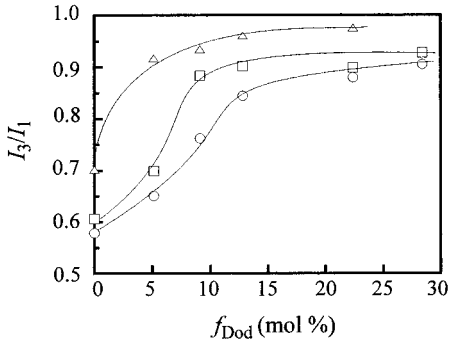

Figure 3. I_3/I_1 ratio for pyrene probes as a function of f_{Dod} at pH 4 (△), 7 (□), and 10 (○) in 0.05 M NaCl aqueous solutions: C_p = 1 g/L.

Figure 3 shows the I_3/I_1 ratios for pyrene probes solubilized in 0.05 M NaCl aqueous solutions of the AA/DodMAm copolymer plotted as a function of f_{Dod}. At pH 10, I_3/I_1 for the reference PAA is ca. 0.58, typical of the value in water, and the ratio increases with increasing f_{Dod}, reaching a maximum value of ca. 0.9 at f_{Dod} = 28.4 mol %. A large part of the increase occurs in an f_{Dod} region of 0−13 mol %. The data in Figure 3 indicate that hydrophobic microdomains are formed to some extent in the copolymer of f_{Dod} = 5.1 mol %, reaching a maximum extent at f_{Dod} = 28.4 mol % at pH 10. At pH 7, the profile of the plot of I_3/I_1 vs f_{Dod} is quite similar to that at pH 10, except I_3/I_1 reaches a plateau value at a lower f_{Dod} near 9.1 mol %. At pH 4, the range of f_{Dod} where I_3/I_1 significantly increases shifts toward lower f_{Dod} values, I_3/I_1 reaching nearly a plateau at f_{Dod} near 5.1 mol %. It is to be noted that I_3/I_1 for PAA at pH 4 is ca. 0.7 and significantly larger than those at pH 7 and 10, indicating that pyrene probes are solubilized to some extent in a collapsed coil of PAA at this low pH. The value of I_3/I_1 at f_{Dod} = 5.1 mol % for pH 4 is ca. 0.91, which is nearly a saturated value for pH 7 and 10. These observations indicate that the hydrophobic association of polymer-bound dodecyl groups occurs more significantly at a lower pH, i.e., at a lower charge density on the polymer chain.

Apparent Critical Micelle Concentration (cmc). Excitation spectra of aqueous solutions of the AA/DodMAm copolymer of f_{Dod} = 9.1 mol % at varying C_p in the presence of 4 × 10^{-7} M pyrene are shown in Figure 4. The spectra show peaks associated with the (0,0) band of pyrene at 334 nm in a low-C_p regime, and the peak shifts to 337 nm in a high-C_p regime. The transition of the peak from 334 to 337 nm occurs in a narrow range of C_p. It is known that the (0,0) absorption maximum of pyrene in water at 334 nm shifts to a longer wavelength when pyrene is solubilized in hydrophobic phases.[33,39] Thus, we estimated the ratio of the intensity at 337 nm to that at 334 nm (I_{337}/I_{334}) and plotted in Figure 5 as a function of C_p for the AA/DodMAm copolymers with f_{Dod} = 9.1 and 28.4 mol %. In the low-C_p regime (<10^{-3} g/L), the I_{337}/I_{334} ratios are practically independent of C_p, but the ratio starts to increase significantly as C_p is increased to a certain level. This observation is indicative of the presence of interpolymer association that starts to occur when C_p is increased to a certain level. This onset of an increase in interpolymer association is somewhat abrupt for the copolymer of f_{Dod} = 28.4 mol % at pH 4 and 7 (Figure 5b), which may allow us to estimate an apparent critical micelle concentration (cmc). Here we define cmc as a polymer concentration at which interpolymer associa-

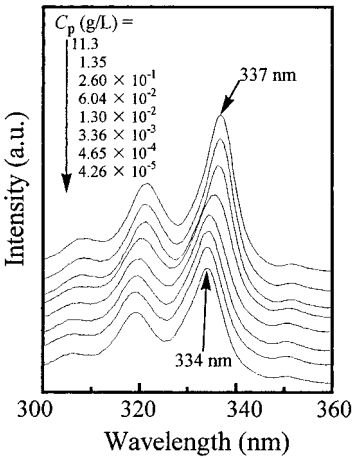

Figure 4. Steady-state fluorescence excitation spectra for pyrene probes solubilized in 0.05 M NaCl aqueous solutions of pH 10 in the presence of the AA/DodMAm copolymer of f_{Dod} = 9.1 mol % at varying polymer concentrations.

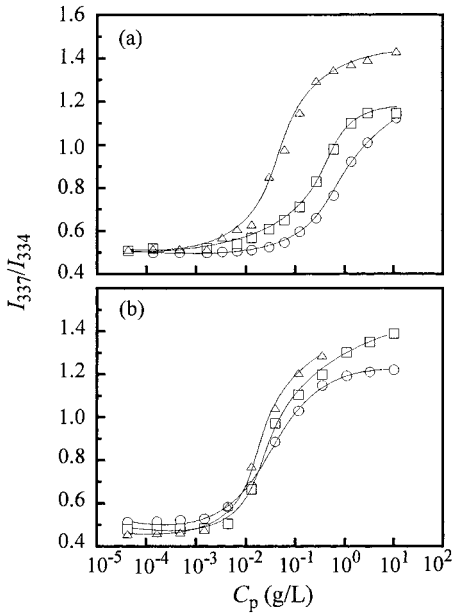

Figure 5. Plots of I_{337}/I_{334} estimated from excitation spectra of the copolymers with f_{Dod} = 9.1 (a) and 28.4 mol % (b) at pH 4 (△), 7 (□), and 10 (○) in 0.05 M NaCl aqueous solutions.

tion starts to occur abruptly. At pH 10, however, I_{337}/I_{334} for the copolymers of f_{Dod} = 28.4 mol % increases gradually. In the case of the copolymer of f_{Dod} = 9.1 mol % (Figure 5a), I_{337}/I_{334} increases more gradually with increasing C_p than for the copolymer of f_{Dod} = 28.4 mol % (Figure 5b) at all pH values. As the DodMAm content is further decreased down to f_{Dod} = 5.1 mol %, I_{337}/I_{334} increases more gradually with increasing C_p (data not shown).

On the basis of the data presented in Figure 5, the ratio of the pyrene concentrations in the hydrophobic phase and in the aqueous phase, $[Py]_m/[Py]_w$, was calculated by assuming the minimum and maximum values of I_{337}/I_{334} at low and high C_p, respectively.[23,24] In Figure 6, $[Py]_m/[Py]_w$ is plotted against C_p for the copolymer of f_{Dod} = 28.4 mol %. At pH 4 and 7, $[Py]_m/[Py]_w$ increases gradually at low C_p and then starts to increase more significantly at a certain C_p value. The gradual increase at low C_p corresponds to an increase in the solubilization of pyrene probes in hydrophobic microdomains formed by intrapolymer associations, and

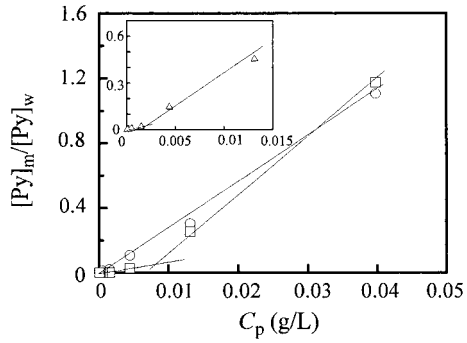

Figure 6. Plots of $[Py]_m/[Py]_w$ calculated on the basis of I_{337}/I_{334} for the AA/DodMAm copolymer of f_{Dod} = 28.4 mol % at pH 4 (△) (inset), 7 (□), and 10 (○) in 0.05 M NaCl aqueous solutions.

the onset of the significant increase in $[Py]_m/[Py]_w$ corresponds to the onset of interpolymer associations to form a multipolymer micelle-like aggregate.[23,24] Therefore, we can regard this onset concentration at a break in the plot as an apparent cmc. The plot for pH 10 shows a straight line passing through the origin without showing a break (Figure 6). Plots for the copolymers with f_{Dod} = 9.1, 12.8, and 22.4 mol % at pH 10 also showed straight lines passing through the origin, and no break was observed (data not shown). These observations suggest that the transition from intrapolymer association to interpolymer association occurs gradually at pH 10 with increasing C_p, exhibiting no clear cmc. Apparent cmc values thus estimated at pH 4 and 7 for the four selected copolymers are listed in Table 1. Values of cmc at pH 4 are smaller than those at pH 7 probably because interpolymer electrostatic repulsion is much less at pH 4 than at pH 7 (Figure 1).

Hydrodynamic Size of Polymer Aggregates. Figure 7 compares relaxation time distributions in QELS measured at a scattering angle of 90° at C_p = 1 g/L in 0.05 M NaCl. Apparent hydrodynamic radii (R_h) were calculated from eq 6 using diffusion coefficients estimated from the linear plot of Γ vs q^2. An R_h value thus calculated for each peak top is indicated in the figure.

At pH 10, the relaxation time distribution for the AA/DodMAm copolymer of f_{Dod} = 5.1 mol % is bimodal. With increasing f_{Dod}, the slow mode peak decreases, relative to the fast mode peak, and the distribution becomes unimodal at f_{Dod} = 28.4 mol %. Furthermore, there is a clear tendency that R_h decreases with increasing f_{Dod}, the copolymer of f_{Dod} = 5.1 mol % showing the largest R_h while the copolymer of f_{Dod} = 28.4 mol % showing the smallest R_h of 5.8 nm at the peak top. This tendency is qualitatively the same as that observed for viscosity (Figure 2). At pH 4, this trend is completely opposite; the relaxation time distribution for the AA/DodMAm copolymer of f_{Dod} = 5.1 mol % is unimodal with R_h = 8.3 nm at the peak top, whereas it becomes bimodal at higher f_{Dod}, and the slow mode peak increases with increasing f_{Dod}.

There appears to be a systematic change in the distribution profile with f_{Dod}. For f_{Dod} = 5.1 and 9.1 mol %, the magnitude of the slow mode peak decreases with decreasing pH, and the distribution becomes apparently unimodal with the peak top shifting toward shorter relaxation times. This indicates that a decrease in polymer charge induces preferential intrapolymer hydrophobic association to form aggregates with smaller R_h in a lower pH region. This trend is completely opposite for the copolymers with $f_{Dod} \geq$ 12.8 mol %; the

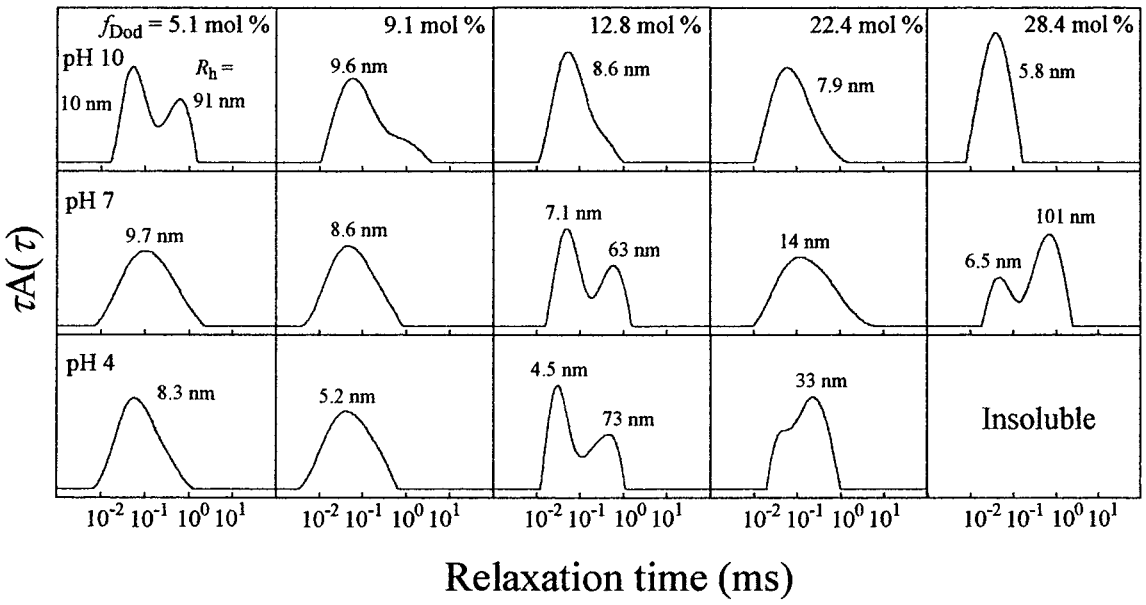

Figure 7. QELS relaxation time distributions for the AA/DodMAm copolymers in 0.05 M NaCl aqueous solutions at C_p = 1 g/L at varying pH values. R_h values corresponding to the relaxation times at peak top are indicated in the figure.

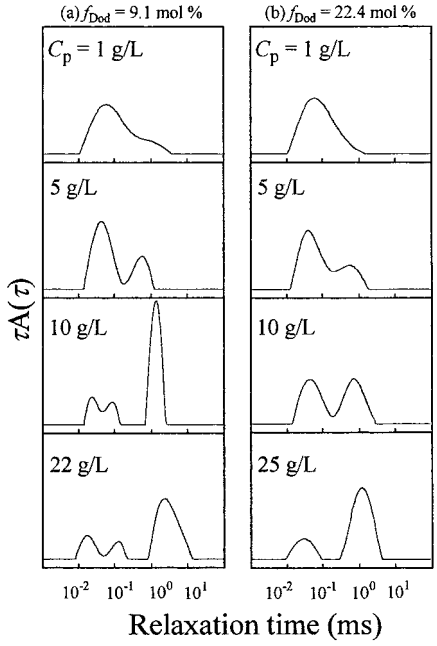

Figure 8. QELS relaxation time distributions for the AA/DodMAm copolymers with f_{Dod} = 9.1 (a) and 22.4 mol % (b) in 0.05 M NaCl aqueous solutions at pH 10 at varying C_p.

magnitude of the slow mode peak increases with decreasing pH, indicating that the interpolymer association of the dodecyl groups occurs more significantly as the polymer charge decreases. From this comparison, one can see that the association behavior of the copolymers with $f_{Dod} \geq$ 12.8 mol % as a function of pH is very different from that of the copolymers with $f_{Dod} \leq$ 9.1 mol %.

Figure 8 compares relaxation time distributions for the copolymers with f_{Dod} = 9.1 and 22.4 mol % at varying C_p at pH 10 in 0.05 M NaCl. With increasing C_p, the slow mode peak increases in magnitude and shifts toward longer relaxation times for both the copolymers, although the relaxation time distributions for the copolymer with f_{Dod} = 9.1 mol % at $C_p \geq$ 10.0 g/L are complicated, exhibiting a multimodal distribution. Apparent R_h values for the peak top of the slow mode are plotted in Figure 9 as a function of C_p. The value of R_h increases with increasing C_p for both the copolymers with f_{Dod} = 9.1 and 22.4 mol %, although the increase is more significant for the former copolymer. These observations indicate that interpolymer association occurs more favorably to form larger aggregates at higher C_p, and this tendency is more significant for the copolymer with lower f_{Dod}.

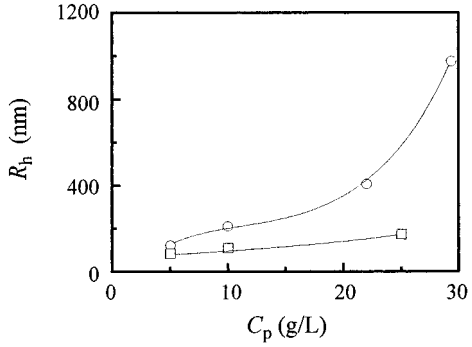

Figure 9. R_h at the slow mode peak top for the AA/DodMAm copolymers with f_{Dod} = 9.1 (○) and 22.4 mol % (□) in 0.05 M NaCl aqueous solutions at pH 10 plotted as a function of C_p.

The value of R_h for the copolymer of f_{Dod} = 9.1 mol % at C_p = 25 g/L is near 1 μm (Figure 9). It should be noted that this R_h value is much larger than the pore size of the membrane filter (0.45 μm in diameter) used to filter sample solutions prior to QELS measurement. This suggests that when the polymer solution is forced to pass through the filter, polymer aggregates are sheared into smaller species so that they can pass through the filter and that they associate back to the original aggregate in the filtrate. In the case of the copolymer of f_{Dod} = 22.4 mol %, the R_h value at C_p = 25 g/L is 174 nm (Figure 9), which is smaller than the pore size of the 0.45 μm filter. However, when the solution was filtered with a membrane filter of a smaller pore size (0.2 μm in diameter), the R_h value decreased to 107 nm (data not shown), suggesting that aggregates with the size larger than the pore size were filtered off. In fact, a decrease in C_p in the filtrate after filtration with the

Table 2. Fitting Parameters for the Infelta−Tachiya Equation and Aggregation Numbers of Dodecyl Groups in One Hydrophobic Microdomain

f_{Dod} (mol %)	pH	[pyrene][a] (μM)	A_3	A_4 ($\times 10^{-6}$ s^{-1})	A_2^{-1} (ns)	χ^2	N_{agg}	av N_{agg}
9.1	10	8.01	0.626	5.64	405	1.03	166	
	7	17.8	0.408	3.76	384	1.10	84	
	4	70.4	0.531	4.16	377	1.11	30	
12.8	10	10.9	0.226	5.57	384	1.00	128	
		8.26	0.214	5.88	384	1.02	132	130
	7	20.4	0.493	3.94	388	1.12	126	
		17.4	0.332	5.62	385	1.15	123	
		13.5	0.341	5.20	380	1.01	127	125
	4	81.5	0.537	3.85	358	1.00	46	
		72.1	0.478	4.28	393	1.13	41	
		59.0	0.424	3.60	371	1.08	37	41
22.4	10	18.1	0.325	5.10	396	1.06	154	
		17.2	0.312	5.31	389	1.02	150	152
	7	36.3	0.578	3.74	406	1.14	125	
		30.4	0.468	3.46	397	1.01	127	
		22.8	0.395	3.45	408	1.13	129	127
28.4	10	52.4	1.050	4.02	408	0.9	162	
		43.2	0.641	4.95	402	1.14	161	
		28.4	0.424	5.55	403	1.30	157	160
	7	82.9	0.468	3.46	397	1.19	93	
		75.6	0.412	4.80	328	1.00	62	78

[a] Calculated from the absorbance at 338 nm using $\epsilon_{338} = 3.7 \times 10^4$ M^{-1} cm^{-1} (ref 32).

0.2 μm filter was confirmed by UV absorption spectroscopy. In the case of the copolymer of $f_{Dod} = 9.1$ mol %, neither a decrease in R_h nor a decrease in C_p after filtration of the solution with the 0.2 μm filter was observed. These observations suggest that the multipolymer aggregates formed from the copolymer of $f_{Dod} = 9.1$ mol % are in equilibrium between disruption and re-formation under shear conditions, but this is not the case for the copolymer of $f_{Dod} = 22.4$ mol %. We will discuss this point in detail in the following subsections.

Aggregation Number of Dodecyl Groups in Microdomain. The mean aggregation number of dodecyl groups in one hydrophobic microdomain (N_{agg}) was determined employing a fluorescence quenching technique based on the excimer formation of pyrene probes solubilized in the hydrophobic microdomain.[17,23,24,35−37,43] Fluorescence of monomeric pyrene is quenched when the concentration of pyrene is relatively high. We confirmed that the excimer formation is only the quenching process for pyrene fluorescence from the fact that fluorescence decays are virtually single-exponential when the concentration of pyrene solubilized in the hydrophobic microdomain is sufficiently low. From single-exponential decay data for the copolymers with $f_{Dod} = 9.1-28.4$ mol % ($C_p = 5$ g/L) measured at a pyrene concentration of 4.0×10^{-7} M at varying pH, fluorescence lifetimes were found to be practically constant at ca. 390 ns independent of pH and f_{Dod}. When the concentration of pyrene was increased to the order of 10^{-5} M, however, the decay profiles became obviously nonexponential. We applied the Infelta−Tachiya kinetics (eq 7)[35−37] to analyze pyrene fluorescence decay data, assuming that all pyrene probes are randomly distributed over the hydrophobic microdomains according to a Poisson distribution. Fluorescence decays were measured at several different concentrations of pyrene at a fixed polymer concentration of 5 g/L (Table 2), and the data were fitted to eq 7. Parameters in eq 7 that resulted in best fits are listed in Table 2 along with calculated N_{agg} values. Values of N_{agg} thus determined are much larger than the numbers of hydrophobes per polymer chain (Table 1). Therefore, it is obvious that each hydrophobic microdomain is comprised of a number of polymer chains.

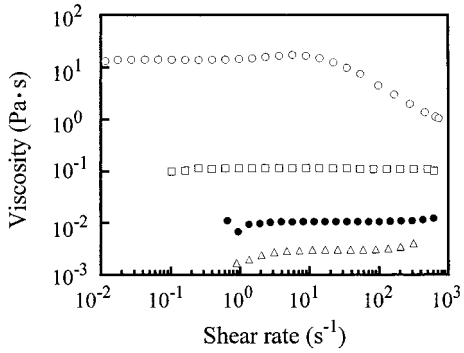

Figure 10. Steady-shear viscosity as a function of shear rate for the AA/DodMAm copolymers with $f_{Dod} = 9.1$ mol % at $C_p = 50$ (□) and 80 g/L (○) and $f_{Dod} = 22.4$ mol % at $C_p = 50$ g/L (△) in 0.05 M NaCl aqueous solutions at 25 °C and pH 10. For comparison, plots for the AMPS/DodMAm copolymer of $f_{Dod} = 10$ mol % at $C_p = 100$ g/L in 0.05 M NaCl aqueous solutions at 25 °C (●) are presented in the figure.

It is important to compare N_{agg} (Table 2) and R_h (Figure 7) as a function of pH. As can be seen in Table 2, N_{agg} decreases with decreasing pH for all f_{Dod}. In the case of the copolymer with $f_{Dod} = 9.1$ mol %, both N_{agg} and R_h decrease as pH is decreased, although the decrease in N_{agg} is much more drastic than the decrease in R_h. In the case of the copolymers with $f_{Dod} \geq 12.8$ mol %, in contrast, the trends of N_{agg} and R_h against pH are opposite, N_{agg} decreasing while R_h increasing with decreasing pH. Namely, a multipolymer aggregate with a larger R_h contains hydrophobic microdomains with a smaller N_{agg}. We will discuss this point in the Discussion section.

Steady-Shear Viscosity in a Concentrated Regime. Steady-shear viscosities of the AA/DodMAm copolymers with $f_{Dod} = 9.1$ and 22.4 mol % in 0.05 M NaCl at pH 10 are plotted in Figure 10 as a function of the shear rate. The viscosity of the AA/DodMAm copolymer of $f_{Dod} = 9.1$ mol % is ca. 2 orders of magnitude higher than that of the copolymer of $f_{Dod} = 22.4$ mol % as compared at $C_p = 50$ g/L. As C_p is increased from 50 to 80 g/L, the viscosity of the AA/DodMAm copolymer of $f_{Dod} = 9.1$ mol % increases by ca. 2 orders of magnitude, and the solution exhibits shear thinning at shear rates higher than ca. 10 s^{-1} at $C_p = 80$ g/L. The viscosity decreases by over 1 order of magnitude as the shear rate is increased from 10 to 10^3 s^{-1}. It appears that the polymer solution exhibits slight shear thickening before the shear thinning starts to occur in a shear rate range of 1−10 s^{-1}. Since shear thickening can be driven by a shear-induced increase in the density of mechanically active chains, a plausible explanation for the observed shear thickening is a shear-induced increase in interpolymer association and hence the size of the polymer aggregate.[41,44] A further increase in the shear rate may cause the multipolymer aggregate to fragment, resulting in a decrease in the size of the multipolymer aggregate and hence a decrease in viscosity.

In Figure 10, viscosity data for an AMPS/DodMAm copolymer of $f_{Dod} = 10$ mol % are also presented for comparison. The M_w estimated by SLS for this AMPS/DodMAm copolymer is 5.0×10^4 as compared with $M_w = 3.2 \times 10^4$ for the AA/DodMAm copolymer of $f_{Dod} = 9.1$ mol %. Although the molecular weights of these two copolymers are similar, the viscosity for the AMPS/

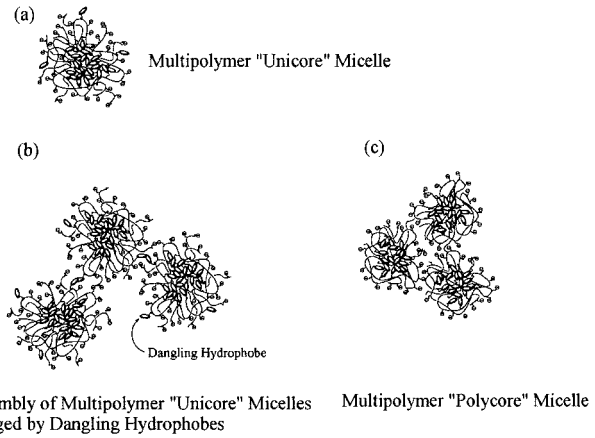

Figure 11. Hypothetical models for multipolymer aggregates formed from the AA/DodMAm copolymers.

DodMAm copolymer at $C_p = 100$ g/L is ca. 1 and 3 orders of magnitude lower than that of the AA/DodMAm copolymer with $f_{Dod} = 9.1$ mol % at $C_p = 50$ and 80 g/L, respectively, comparing in a shear rate region of $1-10$ s^{-1}. In a previous paper,[28] we reported that the AMPS/DodMAm copolymer of $f_{Dod} = 10$ mol % showed unimodal relaxation time distributions in QELS with an R_h value near 5 nm independent of C_p, indicative of predominant intrapolymer association. This striking difference in the association behavior of the AA/DodMAm and AMPS/DodMAm copolymers will be discussed in the following section.

Discussion

The AA/DodMAm copolymer shows a tendency for interpolymer association even in a dilute regime, exhibiting a reasonably well-defined onset of interpolymer associations (i.e., an apparent cmc) at a low C_p at pH 4 and 7. The association behavior depends strongly on both f_{Dod} and pH. At pH 10, the AA/DodMAm copolymer of $f_{Dod} = 28.4$ mol % shows a relatively narrow unimodal distribution in QELS relaxation time with a peak corresponding to $R_h = 5.8$ nm (Figure 7) at $C_p = 1$ g/L. At a glance, one may think that this relatively narrow distribution and small R_h may be an indication of a unimolecular micelle, but this is obviously not the case because N_{agg} for this copolymer at pH 10 is ca. 160 (Table 2), which is ca. 9 times larger than the number of dodecyl groups per polymer chain (Table 1). Therefore, it is clear that a multipolymer aggregate is formed from at least nine polymer chains, assuming that the polymer aggregate contains only one hydrophobic microdomain (i.e., unicore micelle as conceptually illustrated in Figure 11a). This is in sharp contrast to the case of AMPS/DodMAm copolymers that form predominantly unimolecular micelles.[13,20,21,28,29] The AA/DodMAm copolymer of $f_{Dod} = 22.4$ mol % shows apparently unimodal distributions at pH 10 and 7 (Figure 7). If we assume a unicore micelle, the micelle may be formed from ca. 13 and 11 polymer chains at pH 10 and 7, respectively. The AA/DodMAm copolymer of $f_{Dod} = 9.1$ mol % also exhibits apparently unimodal distributions at pH 7 and 4 (Figure 7), and polymer aggregates may be formed from at least eight and three polymer chains at pH 7 and 4, respectively, if unicore micelles are assumed.

As discussed by McCormick and co-workers,[19] for polymers bearing carboxylic acid groups, intrapolymer hydrogen bonding between carboxylic acid groups is an important factor to determine polymer conformation, especially at low pH ($\approx$4). We believe that hydrogen bonding is playing an important role in self-association of the present AA/DodMAm copolymers at pH = 4. At the present time, however, we have no experimental evidence for hydrogen bonding between carboxylic acid groups in the AA/DodMAm copolymers. Thus, the effect of hydrogen bonding on the association behavior of the AA/DodMAm copolymers remains as a subject of our future work.

Two plausible models for the multipolymer aggregates responsible for the slow mode in QELS relaxation time distributions may be speculated as conceptually illustrated in Figure 11b,c. When f_{Dod} is small, all the hydrophobes may not be able to participate in the formation of hydrophobic microdomains because the hydrophobic association can occur only when it prevails over charge repulsion on the same polymer chain or between different chains. This is particularly true at pH 10, at which all the AA units on the polymer chain are fully charged (Figure 1). In this situation, some hydrophobes may fail to be incorporated into hydrophobic microdomains, remaining as dangling hydrophobes. Such dangling hydrophobes may associate together at a higher C_p, yielding a larger aggregate with a network structure (Figure 11b). Since the junction of the network is the association of the dangling hydrophobes, the junction may easily be disrupted under shear conditions. On the other hand, when f_{Dod} is sufficiently high, all hydrophobes may be incorporated in hydrophobic microdomains formed by either intra- or interpolymer association. At high polymer concentrations, interpolymer hydrophobic association is more likely to occur, and hydrophobic microdomains are formed from a large number of different polymer chains, thus yielding a large aggregate with a network structure (Figure 11c). In this type of the polymer network, a number of polymer chains are interconnected by hydrophobic microdomains, and thus the interpolymer junction may not be disrupted as easily as the junction formed by associations of dangling hydrophobes.

As described above, the association behavior of the AA/DodMAm copolymer is markedly different from that of the AMPS/DodMAm copolymer reported in our previous papers,[13,16,20,21,28,29,31] the former showing a tendency for interpolymer association while the latter showing an extremely strong tendency for intrapolymer association. A characteristic difference in the chemical structure between the AA/DodMAm and AMPS/DodMAm copolymers is the distance between the charged group and the polymer backbone (d). In the case of the AA/DodMAm copolymer, the charged groups are located near the polymer backbone ($d = 1.5-2.2$ Å), whereas in the AMPS/DodMAm copolymer, the charged groups are located farther from the polymer main chain ($d = 8.0-9.1$ Å). In addition, as pointed out by McCormick and co-workers,[6] the geminal dimethyl groups in the AMPS repeat unit may be sufficiently hydrophobic to associate with neighboring hydrophobes on the same polymer chain and hence interfere with interpolymer associations of the hydrophobes. If such intrapolymer associations occur between the AMPS unit and dodecyl groups, the polymer chain would be folded into a closed conformation where further intrapolymer polymer associations of dodecyl groups become more favorable.

The hydrophobic interaction of dodecyl groups with the geminal dimethyl groups in the AMPS unit is

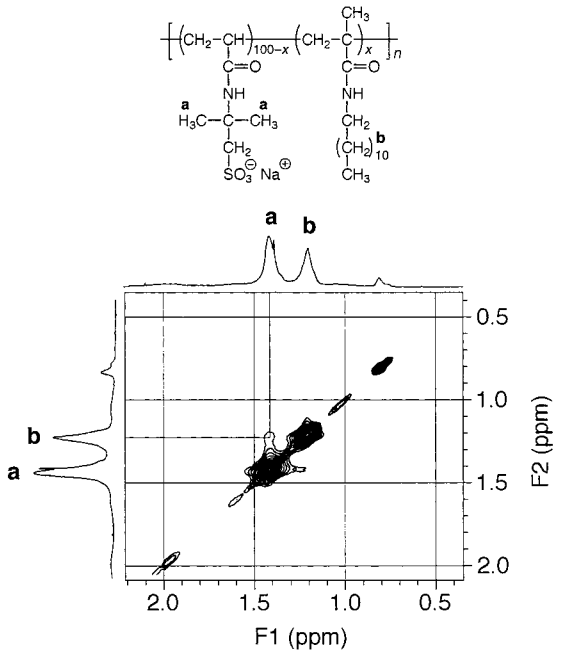

Figure 12. The 600 MHz NOESY spectrum for the AMPS/DodMAm copolymer of f_{Dod} = 20 mol % measured in D_2O at 30 °C.

suggested by nuclear Overhauser effect (NOE) spectroscopy (NOESY). Figure 12 shows an NOESY spectrum for the AMPS/DodMAm copolymer of f_{Dod} = 20 mol % measured in D_2O. The assignments of the peaks are indicated in the figure. Cross-peaks between protons in the geminal dimethyl groups and in the methylene unit in the dodecyl group were observed. Since NOE is due to the transfer of magnetization between protons existing in a length scale of several angstroms with a long motional correlation time, the observed cross-peaks in the NOESY may be regarded as an indication of the presence of hydrophobic interaction between the geminal dimethyl and dodecyl groups in the AMPS/DodMAm copolymer.

Conclusions

The association behavior of random copolymers of AA and DodMAm with f_{Dod} ranging from 5.1 to 28.4 mol % was investigated by fluorescence spectroscopy, QELS, and viscometry in 0.05 M NaCl aqueous solutions at pH 4, 7, and 10. The copolymers showed a strong tendency for interpolymer association depending on f_{Dod} and pH, exhibiting an onset of interpolymer association (i.e., apparent cmc) at pH 4 and 7 at a low C_p on the order of 10^{-3} g/L. At pH 10, the relaxation time distribution in QELS for the copolymer of f_{Dod} = 5.1 mol % was bimodal with a fast mode peak corresponding to an R_h of 10 nm and a slow mode peak to 91 nm. With increasing f_{Dod}, the slow mode peak decreased, relative to the fast mode peak, and the distribution became unimodal at f_{Dod} = 28.4 mol % with a peak corresponding to R_h = 5.8 nm. At pH 4, this trend was opposite. The relaxation time distribution for the copolymer of f_{Dod} = 5.1 mol % was unimodal with R_h = 8.3 nm at the peak top whereas it became bimodal with increasing magnitude of the slow mode peak at higher f_{Dod}. The unimodal distributions observed for lower f_{Dod} at lower pH and those for higher f_{Dod} at higher pH were both due to multipolymer aggregates because the values of N_{agg} of dodecyl groups in one hydrophobic microdomain were found to be much larger than the numbers of dodecyl groups per polymer chain.

The association behavior and the nature of the multipolymer aggregates of the copolymers with $f_{Dod} \leq 9.1$ mol % were quite different from those of $f_{Dod} \geq 12.8$ mol %. For the copolymers with $f_{Dod} \leq 9.1$ mol %, the size of the aggregates decreased with decreasing pH along with the N_{agg}. When $f_{Dod} \geq 12.8$ mol %, in contrast, the size increased with decreasing pH while N_{agg} decreased. The hydrodynamic size of the multipolymer aggregates of the copolymers with f_{Dod} = 9.1 and 22.4 mol % increased significantly with increasing C_p at pH 10. This is much more significant for the copolymer of f_{Dod} = 9.1 mol %; the steady-shear viscosity was ca. 2 orders of magnitude higher than that of the copolymer of f_{Dod} = 22.4 mol % at C_p = 50 g/L. The AA/DodMAm copolymer of f_{Dod} = 9.1 mol % exhibited shear thinning at shear rates higher than ca. 10 s^{-1} at C_p = 80 g/L, indicating that the multipolymer aggregate is more dynamic than those formed from the copolymer of f_{Dod} = 22.4 mol %.

These results were compared with our previous results on the associative behavior of AMPS/DodMAm copolymers that exhibited an extremely strong preference for intrapolymer association forming unimolecular micelles independent of C_p. The strong tendency for intrapolymer association of the AMPS/DodMAm copolymer, as opposed to the AA/DodMAm copolymer, was attributed to the participation of the geminal dimethyl groups in the AMPS repeat unit in hydrophobic associations with neighboring dodecyl groups on the same polymer chain.

On the basis of the results from fluorescence, QELS, and viscometry, multipolymer association models for the AA/DodMAm copolymers were proposed.

Acknowledgment. This work was supported in part by Shorai Foundation for Science and Technology.

References and Notes

(1) Yekta, A.; Duhamel, J.; Brochard, P.; Adiwidjaja, H.; Winnik, M. A. *Macromolecules* **1993**, *26*, 1829−1836.
(2) Zhang, Y.; Wu, C.; Fang, Q.; Zhang, Y.-X. *Macromolecules* **1996**, *29*, 2494−2497.
(3) Li, M.; Jiang, M.; Zhang, Y.-X.; Fang, Q. *Macromolecules* **1997**, *30*, 470−478.
(4) McCormick, C. L.; Middleton, J. C.; Cummins, D. F. *Macromolecules* **1992**, *25*, 1201−1206.
(5) McCormick, C. L.; Elliot, D. L. *Macromolecules* **1986**, *19*, 542−547.
(6) Kathmann, E. E.; White, L. A.; McCormick, C. L. *Macromolecules* **1996**, *29*, 5273−5278.
(7) Newman, J. K.; McCormick, C. L. *Macromolecules* **1994**, *27*, 5114−5122.
(8) Neidlinger, H. H.; Chen, G.-S.; McCormick, C. L. *J. Appl. Polym. Sci.* **1984**, *29*, 713−730.
(9) McCormick, C. L.; Salazar, L. C. *J. Macromol. Sci., Pure Appl. Chem.* **1992**, *A29*, 193−205.
(10) Hu, Y.; Smith, G. L.; Richardson, M. F.; McCormick, C. L. *Macromolecules* **1997**, *30*, 3526−3537.
(11) Hu, Y.; Armentrout, R. S.; McCormick, C. L. *Macromolecules* **1997**, *30*, 3538−3546.
(12) Kramer, M. C.; Welch, C. G.; Steger, J. R.; McCormick, C. L. *Macromolecules* **1995**, *28*, 5248−5254.
(13) Morishima, Y.; Nomura, S.; Ikeda, T.; Seki, M.; Kamachi, M. *Macromolecules* **1995**, *28*, 2874−2881.
(14) Binana-Limbelé, W.; Zana, R. *Macromolecules* **1987**, *20*, 1331−1335.
(15) Binana-Limbelé, W.; Zana, R. *Macromolecules* **1990**, *23*, 2731−2739.
(16) Yamamoto, H.; Tomatsu, I.; Hashidzume, A.; Morishima, Y. *Macromolecules* **2000**, *33*, 7852−7861.
(17) Suwa, M.; Hashidzume, A.; Morishima, Y.; Nakato, T.; Tomida, M. *Macromolecules* **2000**, *33*, 7884−7892.

(18) Chang, Y.; McCormick, C. L. *Macromolecules* **1993**, *26*, 6121−6126.
(19) Branham, K. D.; Snowden, H. S.; McCormick, C. L. *Macromolecules* **1996**, *29*, 254−262.
(20) Yamamoto, H.; Mizusaki, M.; Yoda, K.; Morishima, Y. *Macromolecules* **1998**, *31*, 3588−3594.
(21) Yamamoto, H.; Morishima, Y. *Macromolecules* **1999**, *32*, 7469−7675.
(22) Yusa, S.; Kamachi, M.; Morishima, Y. *Langmuir* **1998**, *14*, 6059−6067.
(23) Noda, T.; Morishima, Y. *Macromolecules* **1999**, *32*, 4631−4640.
(24) Noda, T.; Hashidzume, A.; Morishima, Y. *Macromolecules* **2000**, *33*, 3694−3704.
(25) Noda, T.; Hashidzume, A.; Morishima, Y. *Langmuir* **2000**, *16*, 5324−5332.
(26) Noda, T.; Hashidzume, A.; Morishima, Y. *Macromolecules* **2001**, *34*, 1308−1317.
(27) Morishima, Y. In *Solvents and Self-Organization of Polymers*; Webber, S. E., Tuzar, D., Munk, P., Eds.; Kluwer Academic Publishers: Dordrecht, The Netherlands, 1996; p 331.
(28) Hashidzume, A.; Yamamoto, H.; Mizusaki, M.; Morishima, Y. *Polym. J.* **1999**, *31*, 1009−1014.
(29) Morishima, Y.; Hashidzume, A. Single-Molecular Assemblies of Hydrohobically-Modified Polyelectrolytes and Their Functionalization. In *Specialty Monomers and Polymers. Synthesis, Properties, and Applications*; Havelka, K. O., McCormick, C. L., Eds.; ACS Symposium Series 755; American Chemical Society: Washington, DC, 2000; Chapter 7.
(30) McCormick, C. L.; Blackmon, K. P.; Elliott, D. L. *J. Polym. Sci., Part A: Polym. Chem.* **1986**, *24*, 2619−2634.
(31) Morishima, Y.; Kobayashi, T.; Nozakura, S. *Polym. J.* **1989**, *21*, 267−274.
(32) Vorobyova, O.; Yekta, A.; Winnik, M. A.; Lau, W. *Macromolecules* **1998**, *31*, 8998−9007.
(33) Wilhelm, M.; Zhao, C.-L.; Wang, Y.; Xu, R.; Winnik, M. A.; Mura, J.-L.; Riess, G.; Croucher, M. D. *Macromolecules* **1991**, *24*, 1033−1044.
(34) Jakes, J. *Czech. J. Phys* **1988**, *B38*, 1305−1316.
(35) Infelta, P. P.; Grätzel, M.; Thomas, J. K. *J. Phys. Chem.* **1974**, *78*, 190−195.
(36) Infelta, P. P. *Chem. Phys. Lett.* **1979**, *61*, 88−91.
(37) Tachiya, M. *Chem. Phys. Lett.* **1975**, *33*, 289−292
(38) Kalyanasundaram, K.; Thomas, J. K. *J. Am. Chem. Soc.* **1977**, *99*, 2039−2044.
(39) Astafieva, I.; Zhong, X. F.; Eisenberg, A. *Macromolecules* **1993**, *26*, 7339−7352.
(40) Turro, N. J.; Arora, K. S. *Polymer* **1986**, *27*, 783−796.
(41) Yekta, A.; Xu, B.; Duhamel, J.; Adiwidjaja, H.; Winnik, M. A. *Macromolecules* **1995**, *28*, 956−966.
(42) Cao, T.; Munk, P.; Ramireddy, C.; Tuzar, Z.; Webber, S. E. *Macromolecules* **1991**, *24*, 6300−6305.
(43) Yekta, A.; Aikawa, M.; Turro, N. J. *Chem. Phys. Lett.* **1979**, *63*, 543−548.
(44) Tam, K. C.; Jenkins, R. D.; Winnik, M. A.; Bassett, D. R. *Macromolecules* **1998**, *31*, 4149−4159.

MA010446F